Opto-Electronic Advances

ISSN 2096-4579 CN 51-1781/TN

Ultra-high spectral purity laser derived from weak external distributed perturbation

Laiyang Dang, Ligang Huang, Leilei Shi, Fuhui Li, Guolu Yin, Lei Gao, Tianyi Lan, Yujia Li, Lidan Jiang and Tao Zhu

Citation: Dang LY, Huang LG, Shi LL, Li FH, Yin GL et al. Ultra-high spectral purity laser derived from weak external distributed perturbation. *Opto-Electron Adv*, **6**, 210149(2023).

https://doi.org/10.29026/oea.2023.210149

Received: 4 November 2021; Accepted: 25 February 2022; Published online: 31 August 2022

Related articles

Boron quantum dots all-optical modulator based on efficient photothermal effect

Cong Wang, Qianyuan Chen, Hualong Chen, Jun Liu, Yufeng Song, Jie Liu, Delong Li, Yanqi Ge, Youning Gong, Yupeng Zhang, Han Zhang

Opto-Electronic Advances 2021 **4**, 200032 doi: 10.29026/oea.2021.200032

Highly sensitive and miniature microfiber-based ultrasound sensor for photoacoustic tomography

Liuyang Yang, Yanpeng Li, Fang Fang, Liangye Li, Zhijun Yan, Lin Zhang, Qizhen Sun

Opto-Electronic Advances 2022 **5**, 200076 doi: 10.29026/oea.2022.200076

More related article in Opto-Electron Journals Group website

Opto-Electronic Advances

http://www.oejournal.org/oea

OE_Journal

@OptoElectronAdv

Opto-Electronic Advances

Article

February 2023, Vol. 6, No. 2

DOI: 10.29026/oea.2023.210149

Ultra-high spectral purity laser derived from weak external distributed perturbation

Laiyang Dang†, Ligang Huang†, Leilei Shi†, Fuhui Li, Guolu Yin, Lei Gao, Tianyi Lan, Yujia Li, Lidan Jiang and Tao Zhu*

Ultra-high spectral purity lasers are of considerable research interests in numerous fields such as coherent optical communication, microwave photonics, distributed optical fiber sensing, gravitational wave detection, optical clock, and so on. Herein, to deeply purify laser spectrum with compact size under normal condition, we propose a novel and practical idea to effectively suppress the spontaneous radiation of the laser cavity through weak external distributed perturbation. Subsequently, a laser configuration consisting of a main lasing cavity and an external distributed feedback cavity is proposed. The feedback signal with continuous spatio-temporal phase transition controlled by a distributed feedback structure is injected into the main cavity, which can deeply suppress the coupling rate from the spontaneous radiation to the stimulated emission and extremely purify the laser spectrum. Eventually, an ultra-narrow linewidth on-chip laser system with a side mode suppression ratio greater than 80 dB, an output linewidth of 10 Hz, and a relative intensity noise less than -150 dB/Hz is successfully obtained under normal conditions. The proposed concept in this work provides a new perspective for extreme regulation of laser parameters by using weak external distributed perturbation, which can be valid for various gain-type lasers with wide wavelength bands.

Keywords: high-coherence; weak external distributed perturbation; narrow linewidth; laser

Dang LY, Huang LG, Shi LL, Li FH, Yin GL et al. Ultra-high spectral purity laser derived from weak external distributed perturbation. *Opto-Electron Adv* **6**, 210149 (2023).

Introduction

With the rapid development of optical information technology, high-coherence light source has become the core carrier to promote the development of coherent optical communication[1–4], optical precision measurement[5–8], and signal synthesis[9–11] due to its ultra-long coherent length and superior low phase noise. Moreover, spectrum linewidth acting as one of the critical parameters employed to characterize the coherence of a laser light source has drawn considerable research attention in academia and industry[12–14]. Many laser configurations with feedback structure have been proposed to obtain high-coherence light sources, which mainly includes two types, i.e., optoelectronic circuit feedback[15–17] and optical feedback[18–20]. For the optoelectronic circuit feedback, the coherence improvement mainly depends on the laser frequency stabilization technology that relies on electrical feedback and compensates for the frequency difference between the laser and the reference frequency. This kind of laser frequency stabilization technology has a complex structure and high cost, which is not convenient for large-scale integrated development of lasers. For the optical feedback method, it is usually based on a fixed external cavity up to now, which mainly depends on the

Key Laboratory of Optoelectronic Technology and Systems (Education Ministry of China), Chongqing University, Chongqing 400044, China.
†These authors contributed equally to this work.
*Correspondence: T Zhu, E-mail: zhutao@cqu.edu.cn
Received: 4 November 2021; Accepted: 25 February 2022; Published online: 31 August 2022

Open Access This article is licensed under a Creative Commons Attribution 4.0 International License.
To view a copy of this license, visit http://creativecommons.org/licenses/by/4.0/.
© The Author(s) 2023. Published by Institute of Optics and Electronics, Chinese Academy of Sciences.

increase of cavity length to improve the coherence of the laser source. However, the external feedback from finite feedback surfaces with fixed routes will induce the periodic laser phase jump with the interference between the main cavity laser and the feedback light, which eventually leads the laser to oscillate into multi new longitudinal modes[21,22], and the laser frequency will be sensitive to environmental vibrations[17,23–25], thermal dynamics noise[26–29], and other factors that might restrict further improvements of the laser coherence. It is worth noting that high-Q-microcavity-based feedback with narrowband filtering effect has been extensively investigated, whereas its wavelength selectivity limits the adaptability to the main laser cavity when tuning the wavelength[30,31].

In this work, we propose a compression concept to realize extreme laser spectrum purification under the excitation from a distributed feedback structure. In this type of laser cavity structure, the feedback signal that can continuously tune laser phase, avoiding phase jump, is fed back into the main cavity, which could effectively suppress the coupling strength between the spontaneous radiation and the stimulated emission and eventually deeply compress the linewidth during the laser oscillation. The proposed distributed external feedback can be generated in a scattering optical waveguide with wide operation wavelength range, which can be used for diverse kinds of laser main cavities, such as Fabry-Perot laser, a distributed feedback laser, and distributed Bragg reflector laser. On this basis, we experimentally investigate and verify the proposed compression concept by utilizing an on-chip laser system with an external distributed feedback structure. Eventually, we successfully obtained an ultra-narrow linewidth laser under normal conditions with a side mode suppression ratio (SMSR) of 80 dB, output linewidth of 10 Hz, and a relative intensity noise (RIN) of −152 dB/Hz. The proposed laser structure with distributed feedback affords a new degree of freedom to realize the extreme laser spectrum purification, which also paves the way to extremely controlling laser parameters such as time-frequency and polarization, under condition of controllable coherence.

Theoretical analysis and simulation

The proposed laser configuration consists of the main cavity and an external cavity with distributed feedback characteristics. Compared to the traditional optical feedback, our architecture presents a novel configuration to achieve an extreme laser spectrum purification, as shown in Fig. 1(a). Herein, the main laser cavity with a medium gain generates an initial broadband gain by exploiting the pumping technology. Subsequently, an initial lasing signal outputs from one side of the main cavity to the external feedback cavity after an initial gain oscillation and longitudinal mode competition. The main cavity laser linewidth broadening is due to the energy coupling between the stimulated emission and spontaneous radiation, which leads to the random and cumulative perturbation of the laser frequency in the main cavity and the formation of emission-line broadening. To weaken the coupling strength of spontaneous radiation, the external distributed cavity structure is introduced. The first effect is to increase the cycling time of laser in the main cavity with distributed feedback, which can reduce the noise coupling rate from the spontaneous radiation, and greatly reduce the intrinsic linewidth. The second effect is that the distributed weak feedback can be considered to continuously modify the laser phase in the time domain, because each feedback intensity from a single scattering point is even weaker than the spontaneous radiation, as shown in the inset of Fig. 1(a), which can avoid the phase jump in the time domain as caused by the traditional fixed-cavity feedback that usually forms strong multi-longitudinal mode competition. Therefore, the distributed weak feedback can not only slow down the spontaneous radiation coupling rate, but also have the ability to maintain the laser to the single longitudinal mode operation state. Hence, the phase fluctuation ($\Delta\phi$) and noise coupling strength induced by the spontaneous radiation per cycle in the main cavity are greatly reduced based on the weak distributed feedback, as shown in Fig. 1(b). Consequently, the laser spectrum is highly purified in the phase noise suppression process, as shown in Fig. 1(c).

Based on the proposed laser configuration, we analyze the suppression principle of spontaneous radiation and the optical feedback signal acting as the excitation signal during the laser oscillation. In this process, it is necessary to deeply analyze the characteristics of photon number density in the active cavity. Herein, combined with the optical feedback characteristics from the external cavity possessing the distributed feedback, the simplified two-level rate equation of the photon number density corresponding to the gain oscillation of the proposed laser configuration can be described as[32,33]:

$$\frac{\mathrm{d}N_{\mathrm{m}}(\nu)}{\mathrm{d}t} = \Delta n W_{21}(\nu) + n_2 A_{21}(\nu) + N_{\mathrm{B}}(\nu) - \frac{c\chi N_{\mathrm{m}}(\nu)}{n_{\mathrm{eff}} l}, \tag{1}$$

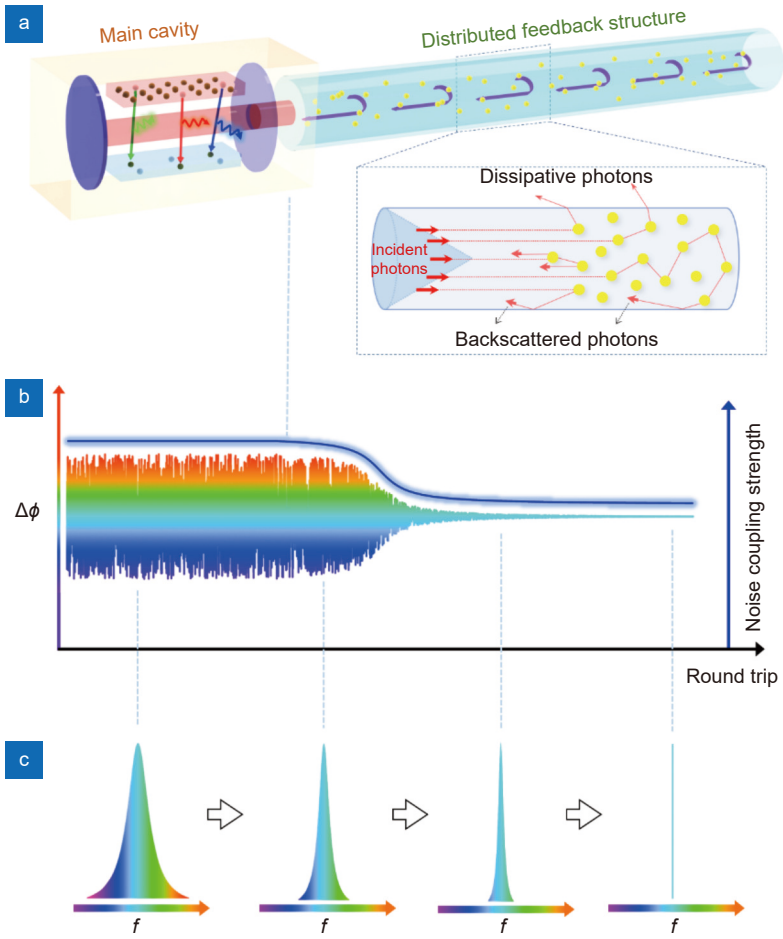

Fig. 1 | Principle of laser spectral purification based on distributed weak perturbation. (**a**) A novel laser configuration. (**b**) Evolution of laser phase fluctuation and noise coupling strength with different round trips. (**c**) Spectral distribution at different noise levels.

where $N_{\rm m}(v)$ denotes the photon density in the main cavity during the operation of the laser, v is the frequency of the laser signal, Δn is the number of reversed-carriers in the energy band, n_2 is the carrier density at lasing energy-level, $W_{21}(v)$ and $A_{21}(v)$ represent the probabilities of stimulated emission and spontaneous radiation from E_2 to E_1, respectively. $N_{\rm B}(v)$ is the photon density corresponding to the feedback-mode signal from the distributed feedback structure, c is the speed of light in vacuum, χ is the single-pass loss of the main cavity, $n_{\rm eff}$ is the effective refractive index of the active cavity, and l is the geometric length of the resonator. Due to the inevitable intrinsic loss of the cavity-mode signal in the distributed feedback structure, the photon density corresponding to the cavity-mode signal traversing a transmission length z from the input terminal can be expressed as:

$$N_z(v) = N_0(v)\exp(-\alpha z), \tag{2}$$

where α denotes the transmission loss coefficient in the feedback structure, $N_0(v)=cTN_{\rm m}(v)/n_{\rm eff}l$ represents the initial photon number density injected into the distributed feedback structure, and T is the transmissivity corresponding to the output end of the main cavity. Based on the above analysis, the feedback photon number density from the dz length within the distributed feedback structure can be described as:

$$\begin{aligned} {\rm d}N_{\rm B}(v) &= N_z(v)\beta\Theta S\exp(-\alpha z)\,{\rm d}z \\ &= N_0(v)\beta\Theta S\exp(-2\alpha z)\,{\rm d}z\,, \end{aligned} \tag{3}$$

where β is the feedback coefficient corresponding to each particle, Θ is the particle concentration on the feedback plane within the distributed feedback structure, and S is the effective area corresponding to each feedback plane. Based on the distribution characteristics of the equivalent feedback plane for the proposed laser structure and the resonant characteristics of the cavity mode signal, the spectral linewidth of the cavity mode signal corresponding to the feedback plane at the z-axis will decrease as the distance for the z value increases. This is due to the change of the effective cavity length attributed to each equivalent feedback plane situated at a different site in

the feedback structure[34–35]. Contrary to the traditional optical feedback method that is based on a fixed cavity, the performance of the main laser cavity would not be influenced by the feedback signal from one or more of the feedback planes. This phenomenon mainly depends on the overall characteristics of the distributed feedback structure. To reveal the resonant characteristics of the cavity mode signal that corresponds to the feedback planes at different sites along the z-axis of the feedback structure, the bandwidth of the cavity mode signal related to the feedback plane at the z-axis, while considering the unidirectional transmission loss, can be expressed as:

$$\Delta\nu_D(z) = \frac{c\left[1-\beta\Theta S\exp(-\alpha z)\right]}{2\pi z}. \tag{4}$$

In our theoretical model, the feedback photon density is caused by the scattering of injected photons by continuously distributed dielectric particles in the distributed feedback structure. Here, we cannot directly treat the distributed feedback signal as the same power that is feedback into the main cavity as the traditional optical feedback. Herein, to further reveal the influence of the overall characteristics of the distributed feedback structure on the improved laser performance, it is necessary to calculate the photon density of the feedback signal accumulated at each point of the feedback structure. Hence, we can express the total feedback photon density injected into the main laser as:

$$\begin{aligned} N_B(\nu) &= \int_0^L N_0(\nu)\beta\Theta S\exp(-2\alpha z)\,\mathrm{d}z \\ &= \frac{N_0(\nu)\beta\Theta S}{2\alpha}\left[1-\exp(-2\alpha L)\right], \end{aligned} \tag{5}$$

where L is the entire length of the feedback structure. If the remaining parameters of the feedback structure are unchanged, the photon density injected into the main laser cavity will be accumulated as the length L of the feedback structure increases. In this situation, based on the distribution characteristics of the particles in the feedback structure, the cavity mode signal matched with the output wavelength of the main cavity will be dominant and act as the required excitation signal for the laser gain to suppress the spontaneous radiation. Herein, the corresponding spontaneous radiation rate has been deeply analyzed when the laser is oscillating stably ($\mathrm{d}N_m(\nu)/\mathrm{d}t=0$), which can be expressed as follows:

$$\begin{aligned} R_{21}(\nu) &= n_2A_{21}(\nu) \\ &= \frac{c\chi N_m(\nu)}{n_{\mathrm{eff}}l} - N_B(\nu) - \Delta nW_{21}(\nu). \end{aligned} \tag{6}$$

The spontaneous radiation rate $R_{21}(\nu)$ would be suppressed with the increase of the photon number density $N_B(\nu)$ of the cavity mode signal injected into the main laser cavity. The phase fluctuations of the optical field caused by the spontaneous radiation would be the main factor for the intrinsic linewidth[36]. This shows that effectively suppressing the spontaneous radiation by utilizing the external feedback signal is fundamental to realizing extreme laser linewidth compression. Based on the above analysis, the laser linewidth equation, which is modified due to the presence of the feedback signal from the distributed feedback structure, can be expressed as:

$$\begin{aligned} \Delta\nu &= \frac{1+\eta^2}{4\pi N_m}\int_{-\infty}^{\infty}R_{21}(\nu)\mathrm{d}\nu \\ &= \frac{c(1+\eta^2)}{4\pi n_{\mathrm{eff}}}\left\{\frac{\chi}{l}-g-\frac{T\beta\Theta S}{2\alpha l}\left[1-\exp(-2\alpha L)\right]\right\}, \end{aligned} \tag{7}$$

where η represents the linewidth enhancement factor, $N_m=\int_{-\infty}^{\infty}N_m(\nu)\mathrm{d}\nu$ the total photon density in the main cavity, $g=\int_{-\infty}^{\infty}\Delta n\sigma_{21}(\nu)\mathrm{d}\nu$ the gain factor, and $\sigma_{21}(\nu)$ the emission cross-section of each frequency mode. The stimulated emission probability can be expressed as $W_{21}(\nu)=cN_m\sigma_{21}(\nu)/n_{\mathrm{eff}}$ for the homogeneous broadening medium. The proposed laser structure is essential to realize the laser linewidth deep compression by effectively controlling the photon number density from the distributed feedback structure.

To validate our analysis, we conduct the simulation illustrated in Fig. 2. The laser linewidth evolution based on distributed external feedback as a function of the feedback structure under different feedback coefficients is illustrated in Fig. 2(a). Herein, it can be deduced that the laser linewidth can be compressed with the feedback length and coefficient increase. In addition, in order to theoretically verify the trade-off between the photon number density of the main cavity and the feedback structure, the laser output linewidth is calculated for different feedback ratios as shown in Fig. 2(b). Figure 2(c) demonstrates the interplay between the laser linewidth compression law and length L's distributed feedback structure when the feedback coefficient β_4=1.5 ×10^{-4}, where the brightness of the curve color marks the spectral linewidth. In principle, the output spectrum becomes narrower as the length increases, thereby presenting a sharp compression for the output spectrum in the length range of 30 m. Subsequently, the linewidth gradually tends to be an ideal state at a slow rate, suggesting

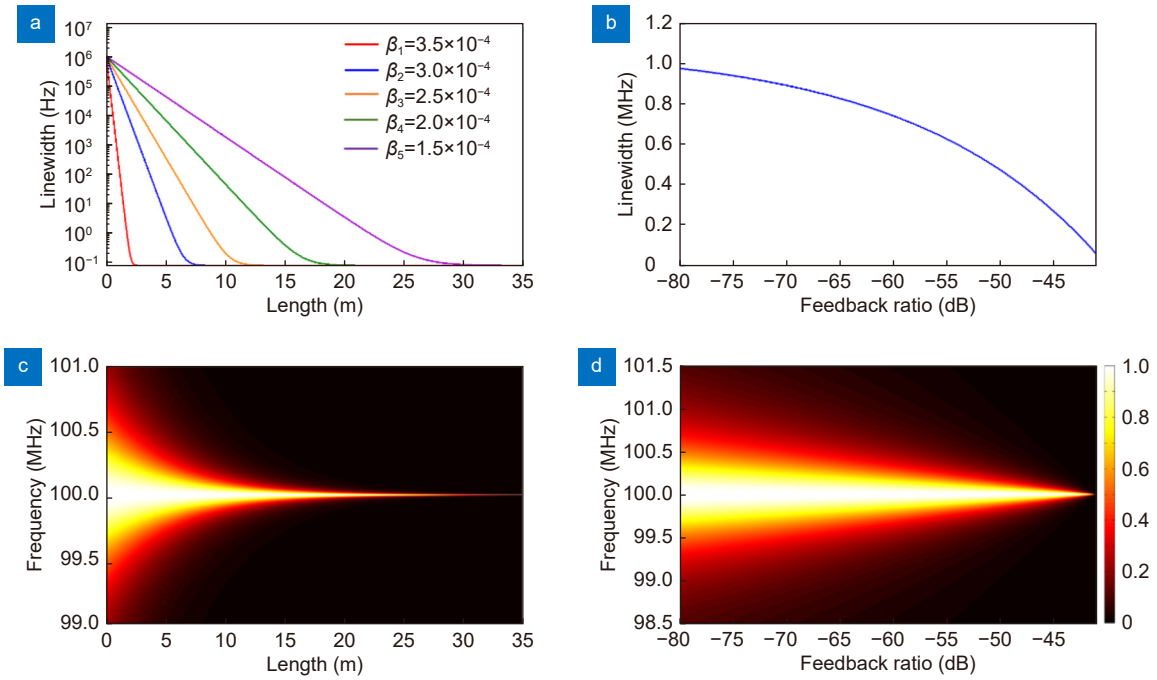

Fig. 2 | Simulation results of laser linewidth evolution. (**a**) Output linewidth evolution with the feedback length under different feedback coefficients. (**b**) Linewidth curve at the different feedback ratios. Two-dimensional pseudocolor maps of the spectra vary (**c**) with the length and (**d**) with feedback ratio.

that the cavity-mode signal from the distributed feedback structure plays the role of the optical power feedback and realizes a deep compression of the laser linewidth by suppressing the spontaneous radiation during the laser oscillation. Figure 2(d) illustrates the variation characteristics of the laser linewidth at different feedback ratios. Similarly, the output spectrum is indicated by the brightness of the curve color, where it is evident that as the feedback ratio increases, the spectrum becomes narrower. This phenomenon suggests that the size of the distributed feedback structure can be reduced by mainly enhancing the feedback coefficient. Therefore, an artificial waveguide structure with high feedback coefficient can be designed to reduce the feedback length in the case of an equivalent frequency spectrum purification. In this way, the laser system based on a distributed feedback scheme can further develop in the direction of miniaturization. At the same time, it is convenient to mitigate the influence of external noise from the environment that acts on the laser. Compared with the conventional optical feedback based on a fixed cavity[37–39], the proposed laser configuration assisted by the distributed feedback can attain extreme laser linewidth compression. This is feasible by providing a cavity mode signal that coincides with the wavelength of the main cavity to suppress the spontaneous radiation effectively. In principle, as long as the spontaneous radiation in the laser gain medium is completely suppressed, the laser can exhibit an ideal monochromatic output.

Experimental step

To verify the proposed laser linewidth compression concept, we propose an on-chip laser system based on a distributed feedback external cavity. The structure is presented in Fig. 3 and primarily consists of the main laser cavity and an external distributed feedback structure. Here, a waveguide structure with appropriate length and feedback coefficient can be used as an external cavity to deeply compress the linewidth, such as an optical fiber, microstructure waveguide, whispering-gallery-mode (WGM) resonator, and so on. The feedback distribution should be as continuous as possible to ensure the continuity of the feedback phase, so as to ensure that the resonant energy with the main cavity laser frequency always exists and could be accumulated. It is worth noting that the distributed feedback from the WGM resonator forms significant filtering effect, which weakens the wavelength adaptability to follow the main laser cavity frequency. The main laser cavity is driven by current to provide an initial optical signal with an output linewidth of megahertz magnitude. The main cavity emits a signal which is injected into the distributed

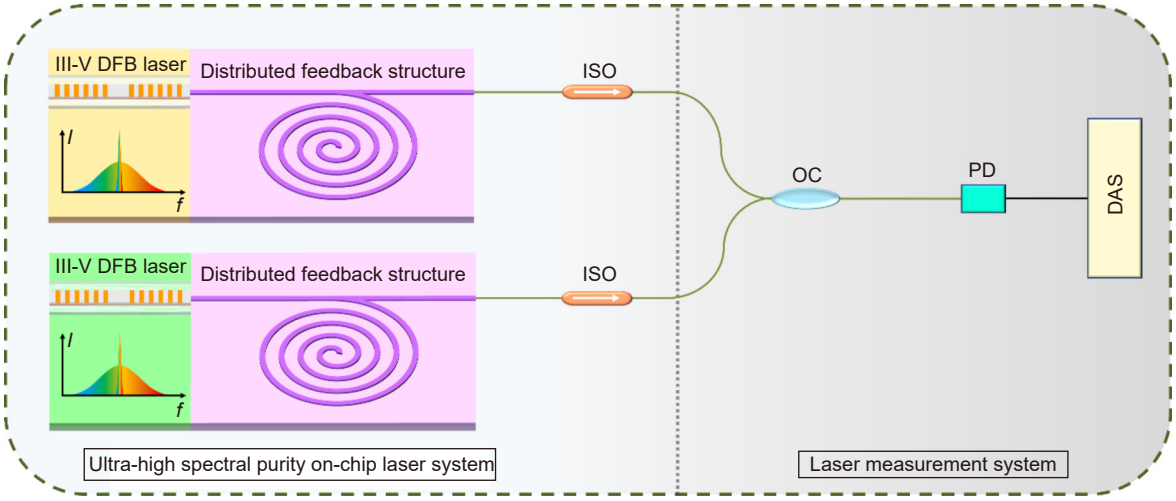

Fig. 3 | An on-chip laser system based on weak external distributed perturbation. ISO: optical isolator; OC: optical coupler; PD: photoelectric detector; DAS: data acquisition system.

feedback structure via a beam splitter, wherein a cavity mode signal matched with the lasing wavelength is formed and fed back into the main cavity to provide an excitation signal required by the laser gain. We utilized an optical isolator (ISO) to mitigate the influence of reflection from the measurement system. Due to the suppression of spontaneous radiation in the laser gain process by a feedback signal from the distributed feedback structure, an ultra-narrow linewidth laser will be obtained eventually. In addition, to ensure the accuracy of characterizing the output laser, we employ a frequency noise measurement method based on differential phase demodulation, and a beat frequency method by exploiting two lasers with the same parameters.

Experimental results and discussion

Based on the proposed laser system, the experimental results are shown in Fig. 4. Two identical lasers have been built to directly demonstrate the ultra-narrow characteristics of the laser-assisted by the distributed feedback. A real-time oscilloscope with a bandwidth of 20 GHz measures the beat-frequency signal between the two lasers with the corresponding signal presented in Fig. 4(a). In the figure, the electric spectrum that corresponds to the free-running DFB laser and the laser-assisted by a feedback power ratio of –45 dB are illustrated by blue and red curves, respectively. The spectral linewidth of the red curve is much smaller than that of the blue curve. Moreover, an SMSR ≥ 80 dB is demonstrated from the curve in a span of 40 MHz. As highlighted in Fig. 4(b), the fitting result of the output linewidth corresponding to the red curve in Fig. 4(a) is approximately 10 Hz. It is worth noting that such a linewidth value has managed to maintain a top-level state-of-the-art performance under a room-temperature condition (the current minimum integral linewidth is about 25 Hz[40]). Compared to the free-running DFB laser linewidth, the linewidth of the proposed method is successfully compressed by five orders of magnitude. The frequency noise power spectral density (PSD) spectrum is then obtained with the demodulated transient frequency by fast Fourier transformation (FFT), as shown in Fig. 4(c). Herein, the frequency noise PSD corresponding to the free-running DFB laser and the laser-assisted by distributed feedback is indicated by black and red curves, respectively. The white noise floor (red curve) is suppressed by 70 dB compared with that of the black curve, and it is approaching sub-Hz^2/Hz magnitude, which suggests that the output linewidth is about several Hz. In addition, the measurement noise floor (gray curve) and white noise floor (red curve) almost coincide, indicating that the linewidth is approximately approaching the measurement limit. To further demonstrate the stability of the distributed feedback laser structure, we measure the relative intensity noise. The corresponding results are illustrated in Fig. 4(d), in which the red and blue curves representing the RIN spectrum result with and without distributed feedback. Figure 4(d) demonstrates that the RIN spectrum (red curve) is suppressed by 20 dB, suggesting that the influence from external disturbances can be suppressed by the feedback signal that coincides with the wavelength of the main cavity in this laser configuration. Consequently, the measured RIN floor is below –155 dB/Hz in the frequency range over 3 MHz.

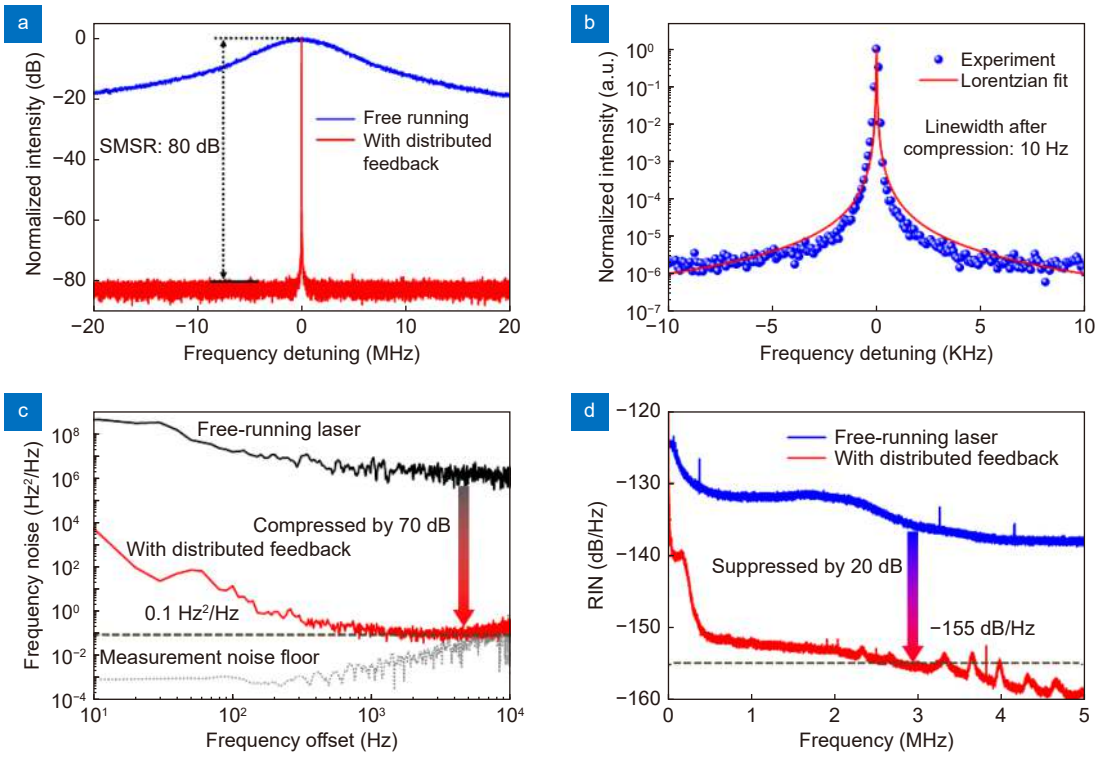

Fig. 4 | Power spectra of the RF signal generated by beating two distributed feedback DFB lasers and spectral purity. (**a**) Comparison curves of the frequency spectrum from beat frequency signal. (**b**) Lorentz fitting curve of the linewidth with a distributed feedback. (**c**) Comparison curves of the frequency noise PSD. (**d**) Comparison curves of the RIN spectrum, where a red curve indicates the compressed result.

We further reveal the influence of the feedback ratio from the distributed feedback structure on the laser output characteristics, with the corresponding experimental results illustrated in Fig. 5. Herein, the feedback ratio is varied by controlling the length of the feedback structure. The frequency noise PSD curves measured under the different feedback ratios are shown in Fig. 5(a), demonstrating that the frequency noise floor within the white noise area around 10 kHz gradually varies from the 10^6 Hz to the sub-Hz order. The latter indicates that the intrinsic laser linewidth, which determines the Lorentzian shape, decreases as the feedback ratio increases. The corresponding Lorentzian linewidth variation curve is illustrated in Fig. 5(b). The last plot confirms the theory, as the inherent laser frequency noise can be well restricted with more robust distributed feedback.

Figure 6 presents the dynamic process of the self-adaptive laser linewidth compression. In Fig. 6(a), we observe that when an electro-optic modulator switches on the feedback, the transient spectrum is extremely compressed with time, especially in the range indicated by the yellow curve. The corresponding Lorentzian linewidth is presented in Fig. 6(b), demonstrating that the linewidth is sharply compressed from the MHz to the 10-Hz order in a time range of 1.1 ms. This shows that the transition time of the laser from the free-running state to the compression state is on the order of milliseconds. To further reveal the adaptive compression characteristics of the proposed laser configuration for different wavelengths, we investigate the dynamic process of the output spectrum in the switching process of the main cavity wavelength by precisely tuning the temperature of the laser diode. Fig. 6(c) and 6(d) demonstrate the transient spectrum and the corresponding Lorentzian linewidth while switching the frequency of the main laser cavity. The frequency switching time is Δt=2.5 ms, which contains three processes, i.e., decompression, free running, and recompression. Herein, the switching time between two steady states depends on the two processes, i.e., the frequency-changing and linewidth-narrowing. The process of modifying the temperature of the laser diode is a dominant contributing factor to the relatively long switching time. Therefore, the adaptive process can be further shortened by speeding up the frequency-changing process. Figure 6 suggests that the linewidth increases sharply when the main laser feedback cavity signal is detuning, indicating that the feedback signal matched with the wavelength of the main cavity plays

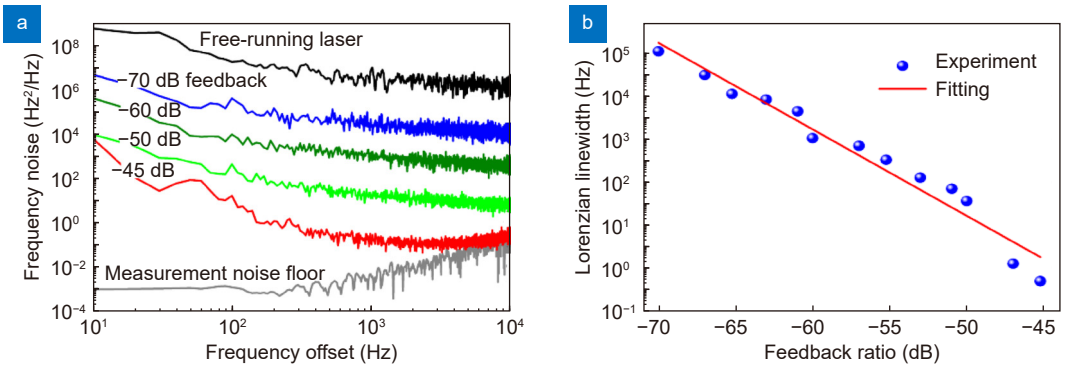

Fig. 5 | Coherence of on-chip laser with different feedback ratios. (**a**) Evolution curves of the frequency noise PSD under different feedback ratios. (**b**) Evolution curves of output linewidth with the feedback ratio.

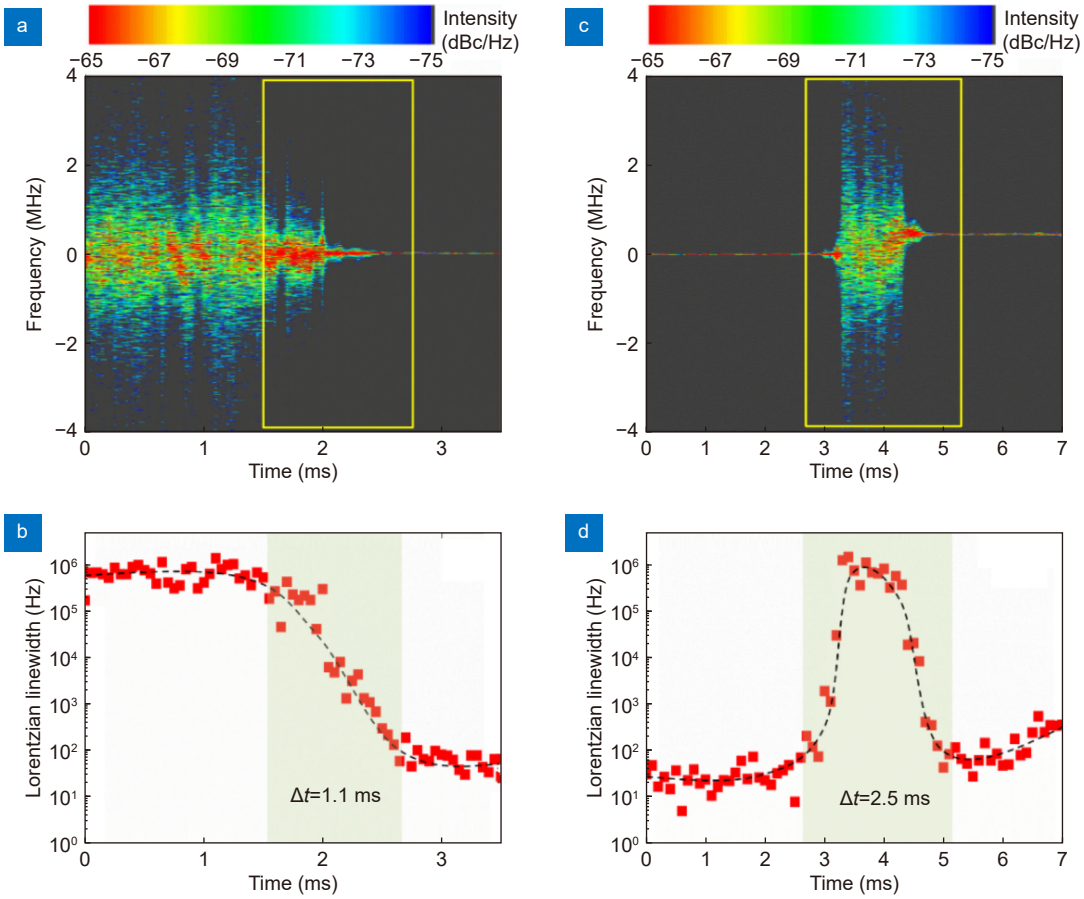

Fig. 6 | Self-adaptive compression process of laser linewidth. (**a**) Transient spectrum and (**b**) corresponding Lorentzian linewidth when switching on the feedback. (**c**) Transient spectrum and (**d**) corresponding Lorentzian linewidth when tuning the frequency of the main laser cavity.

a decisive role in extreme laser linewidth compression. Overall, our findings demonstrate adaptive compression characteristics from the distributed feedback.

The proposed compression concept relying on a weak external distributed perturbation creates a new perspective to obtain ultra-high coherent light sources and further extremely control multi laser parameters of time-frequency and polarization. It is desirable to compress the integral linewidth to sub-Hz level, when inserting the entire laser system into a vacuum with low temperature for extreme thermostatic and vibration isolation in the future work. To improve the tuning performance of the proposed laser structure, the dynamic response of the gain medium and feedback distribution feature needs to be further studied.

Conclusion

In conclusion, we propose a laser spectrum purification

scheme of main cavity with external distributed feedback structure, which can greatly enhance the laser coherence. In this type of laser cavity structure, the distributed feedback signal could effectively suppress spontaneous radiation and deeply compress the linewidth during the laser oscillation. In the experiment, we verify the proposed compression concept by utilizing an on-chip laser system with a weak external distributed feedback structure. Under normal conditions, we obtain an ultra-high spectrum purity laser with an SMSR of 80 dB, output linewidth of 10 Hz, and a RIN of –152 dB/Hz at 1 MHz frequency offset. Also, we reveal the adaptive purification characteristics of the proposed laser configuration for different output wavelengths, by investigating the transient aspects of the output spectrum while switching the laser wavelength. The proposed concept and laser configuration create a new perspective for improving and obtaining high coherence laser sources, which is also of great significance for extremely controlling diverse laser parameters such as time-frequency and polarization.

References

1. Roos C, Zeiger T, Rohde H, Nägerl HC, Eschner J et al. Quantum state engineering on an optical transition and decoherence in a Paul trap. *Phys Rev Lett* **83**, 4713–4716 (1999).
2. Coddington I, Swann WC, Lorini L, Bergquist JC, Le Coq Y et al. Coherent optical link over hundreds of metres and hundreds of terahertz with subfemtosecond timing jitter. *Nat Photonics* **1**, 283–287 (2007).
3. Ip E, Lau APT, Barros DJF, Kahn JM. Coherent detection in optical fiber systems. *Opt Express* **16**, 753–791 (2008).
4. Wang C, Chen QY, Chen HL, Liu J, Song Y F et al. Boron quantum dots all-optical modulator based on efficient photothermal effect. *Opto-Electron Adv* **4**, 200032 (2021).
5. Kwee P, Bogan C, Danzmann K, Frede M, Kim H et al. Stabilized high-power laser system for the gravitational wave detector advanced LIGO. *Opt Express* **20**, 10617–10634 (2012).
6. Maze JR, Stanwix PL, Hodges JS, Hong S, Taylor JM et al. Nanoscale magnetic sensing with an individual electronic spin in diamond. *Nature* **455**, 644–647 (2008).
7. Passy R, Gisin N, von der Weid JP, Gilgen HH. Experimental and theoretical investigations of coherent OFDR with semiconductor laser sources. *J Lightw Technol* **12**, 1622–1630 (1994).
8. Claus D, Alekseenko I, Grabherr M, Pedrini G, Hibst R. Snapshot topography measurement via dual-VCSEL and dual wavelength digital holographic interferometry. *Light Adv Manuf* **2**, 29 (2021).
9. Preu S, Döhler GH, Malzer S, Wang LJ, Gossard AC. Tunable, continuous-wave Terahertz photomixer sources and applications. *J Appl Phys* **109**, 061301 (2011).
10. Yu CX, Augst SJ, Redmond SM, Goldizen KC, Murphy DV et al. Coherent combining of a 4 kW, eight-element fiber amplifier array. *Opt Lett* **36**, 2686–2688 (2011).
11. Ma YX, Wang XL, Leng JY, Xiao H, Dong XL et al. Coherent beam combination of 1.08 kW fiber amplifier array using single frequency dithering technique. *Opt Lett* **36**, 951–953 (2011).
12. Ludlow AD, Boyd MM, Ye J, Peik E, Schmidt PO. Optical atomic clocks. *Rev Mod Phys* **87**, 637–701 (2015).
13. Barwood GP, Huang G, Klein HA, Johnson LAM, King SA et al. Agreement between two $^{88}Sr^{+}$ optical clocks to 4 parts in 10^{17}. *Phys Rev A* **89**, 050501 (2014).
14. Cygan A, Lisak D, Morzyński P, Bober M, Zawada M et al. Cavity mode-width spectroscopy with widely tunable ultra narrow laser. *Opt Express* **21**, 29744–29754 (2013).
15. Stern B, Ji XC, Dutt A, Lipson M. Compact narrow-linewidth integrated laser based on a low-loss silicon nitride ring resonator. *Opt Lett* **42**, 4541–4544 (2017).
16. Spirin VV, Escobedo JLB, Korobko DA, Mégret P, Fotiadi AA. Stabilizing DFB laser injection-locked to an external fiber-optic ring resonator. *Opt Express* **28**, 478–484 (2020).
17. Kessler T, Hagemann C, Grebing C, Legero T, Sterr U et al. A sub-40-mHz-linewidth laser based on a silicon single-crystal optical cavity. *Nat Photonics* **6**, 687–692 (2012).
18. Zhang AQ, Feng XH, Wan MG, Li ZH, Guan BO. Tunable single frequency fiber laser based on FP-LD injection locking. *Opt Express* **21**, 12874–12880 (2013).
19. Brunner D, Luna R, Latorre ADI, Porte X, Fischer I. Semiconductor laser linewidth reduction by six orders of magnitude via delayed optical feedback. *Opt Lett* **42**, 163–166 (2017).
20. Zhao Y, Peng Y, Yang T, Li Y, Wang Q et al. External cavity diode laser with kilohertz linewidth by a monolithic folded Fabry–Perot cavity optical feedback. *Opt Lett* **36**, 34–36 (2011).
21. Lewoczko-Adamczyk W, Pyrlik C, Häger J, Schwertfeger S, Wicht A et al. Ultra-narrow linewidth DFB-laser with optical feedback from a monolithic confocal Fabry-Perot cavity. *Opt Express* **23**, 9705–9709 (2015).
22. Komljenovic T, Srinivasan S, Norberg E, Davenport M, Fish G et al. Widely tunable narrow-linewidth monolithically integrated external-cavity semiconductor lasers. *IEEE J Sel Top Quantum Electron* **21**, 1501909 (2015).
23. Ludlow AD, Huang X, Notcutt M, Zanon-Willette T, Foreman SM et al. Compact, thermal-noise-limited optical cavity for diode laser stabilization at 1×10^{-15}. *Opt Lett* **32**, 641–643 (2007).
24. Webster SA, Oxborrow M, Gill P. Vibration insensitive optical cavity. *Phys Rev A* **75**, 011801 (2007).
25. Millo J, Magalhães DV, Mandache C, Le Coq Y, English EML et al. Ultrastable lasers based on vibration insensitive cavities. *Phys Rev A* **79**, 053829 (2009).
26. Numata K, Kemery A, Camp J. Thermal-noise limit in the frequency stabilization of lasers with rigid cavities. *Phys Rev Lett* **93**, 250602 (2004).
27. Jiang YY, Ludlow AD, Lemke ND, Fox RW, Sherman JA et al. Making optical atomic clocks more stable with 10^{-16}-level laser stabilization. *Nat Photonics* **5**, 158–161 (2011).
28. Nicolodi D, Argence B, Zhang W, Le Targat R, Santarelli G et al. Spectral purity transfer between optical wavelengths at the 10^{-18} level. *Nat Photonics* **8**, 219–223 (2014).
29. Huang H, Duan J, Dong B, Norman J, Jung D et al. Epitaxial quantum dot lasers on silicon with high thermal stability and strong resistance to optical feedback. *APL Photonics* **5**, 016103 (2020).
30. Liang W, Ilchenko VS, Eliyahu D, Savchenkov AA, Matsko AB et al. Ultralow noise miniature external cavity semiconductor

laser. *Nat Commun* **6**, 7371 (2015).
31. Jin W, Yang QF, Chang L, Shen BQ, Wang HM et al. Hertz-linewidth semiconductor lasers using CMOS-ready ultra-high-Q microresonators. *Nat Photonics* **15**, 346–353 (2021).
32. Wong YL, Carroll JE. A travelling-wave rate equation analysis for semiconductor lasers. *Solid State Electron* **30**, 13–19 (1987).
33. Cassidy DT. Comparison of rate-equation and Fabry-Perot approaches to modeling a diode laser. *Appl Opt* **22**, 3321–3326 (1983).
34. Lau EK, Lakhani A, Tucker RS, Wu MC. Enhanced modulation bandwidth of nanocavity light emitting devices. *Opt Express* **17**, 7790–7799 (2009).
35. Li FH, Lan TY, Huang LG, Ikechukwu IP, Liu WM et al. Spectrum evolution of Rayleigh backscattering in one-dimensional waveguide. *Opto-Electron Adv* **2**, 190012 (2019).
36. Henry CH. Theory of the linewidth of semiconductor lasers. *IEEE J Quantum Electron* **18**, 259–264 (1982).
37. Li H, Abraham NB. Power spectrum of frequency noise of semiconductor lasers with optical feedback from a high-finesse resonator. *Appl Phys Lett* **53**, 2257–2259 (1988).
38. Laurent P, Clairon A, Breant C. Frequency noise analysis of optically self-locked diode lasers. *IEEE J Quantum Electron* **25**, 1131–1142 (1989).
39. Huang X, Zhao QL, Lin W, Li C, Yang CS et al. Linewidth suppression mechanism of self-injection locked single-frequency fiber laser. *Opt Express* **24**, 18907–18916 (2016).
40. Lim J, Savchenkov AA, Dale E, Liang W, Eliyahu D et al. Chasing the thermodynamical noise limit in whispering-gallery-mode resonators for ultrastable laser frequency stabilization. *Nat Commun* **8**, 8 (2017).

Acknowledgements

This work was supported by the National Natural Science Foundation of China (NSFC) (61635004), the National Science Fund for Distinguished Young Scholars (61825501), the Chongqing Natural Science Foundation of Innovative Research Groups under Grant (CSTC2020JCYJ, CXTTX0005).

Author contributions

T. Zhu conceived the idea of laser linewidth compression and supervised the project. L. Y. Dang, F. H. Li, and L. G. Huang contributed to the design of the laser system. L. Y. Dang and F. H. Li performed theoretical simulations and provided theoretical support. Measurements were performed by L. Y. Dang, F. H. Li, L. G. Huang, and T. Y. Lan with assistance from G. L. Yin, L. L. Shi, L. Gao, Y. J. Li and L. D. Jiang Analysis of the results was conducted by L. Y. Dang, F. H. Li, L. G. Huang, L. L. Shi, G. L. Yin, and T. Zhu. The manuscript was written by L. Y. Dang, F. H. Li, L. G. Huang, and L. L. Shi with input from all other authors.

Competing interests

The authors declare no competing financial interests.